2023 62nd IEEE Conference on Decision and Control (CDC)
December 13-15, 2023. Marina Bay Sands, Singapore

An error-triggered adaptive model reduction and soil moisture estimation for agro-hydrological system

Sarupa Debnath, Soumya Ranjan Sahoo, Bernard Twum Agyeman, Xunyuan Yin, and Jinfeng Liu

Abstract— **Implementing a closed-loop irrigation system requires an accurate estimation of soil moisture given a limited number of sensors. However, the main challenge lies in the potential high dimensionality (10^4-10^8) of the agro-hydrological model used for water dynamics, which is modeled based on the nonlinear Richards equation. To address this challenge, we propose a state estimation method for large-scale agricultural fields. Our approach uses an error-triggered adaptive model reduction utilizing a trajectory-based clustering technique. An adaptive extended Kalman filter (EKF) is designed accordingly based on the adaptive reduced model. We apply this to an actual agricultural field and conduct extensive simulations to demonstrate its effectiveness and applicability.**

I. INTRODUCTION

Agriculture exerts a significant influence on global freshwater and land usage decisions, with increasing population growth and climate change exacerbating water scarcity. Notably, agricultural irrigation accounts for nearly 70% of annual freshwater consumption [1], with the average water-use efficiency of irrigation methods being only 50-60% [2]. FAOSTAT [3] data shows that agriculture utilizes 38% of the world's land surface, with one-third being cropland. As the global population continues to expand, the demand for cropland intensifies, which further leads to more irrigation water consumption. Therefore, enhancing water-use efficiency in the agricultural sector is an urgent priority for addressing the water crisis.

Currently, open-loop irrigation methods are commonly used in agriculture, where irrigation policies are established based on empirical or heuristic knowledge rather than real-time feedback from the field. This can result in over or insufficient irrigation, which can be avoided by implementing closed-loop irrigation. Closed-loop irrigation takes into account real-time soil moisture information from the field and determines the necessary water quantity, leading to significant improvements in water-use efficiency [4]. However, due to the limited availability of soil sensors, soil moisture can only be monitored in certain locations of a large field. This limited knowledge of soil moisture, combined with the high dimensionality of the agro-hydrological system, presents two major challenges. To address these challenges, model reduction-based state estimation can be an effective approach.

Various state estimation algorithms have been developed, including those based on model reduction. For example, in [5], a state estimation method for wastewater treatment plants using proper orthogonal decomposition (POD) model reduction was proposed. In another study [6], a reduced model was developed by selecting relevant inputs and outputs and the method was applied to estimate states of a reactor-separator system. Pertaining to soil moisture estimation of large-scale agro-hydrological systems, a structure-preserving cluster-based model reduction approach that preserves essential dynamic properties and physical topology, in contrast to POD, was proposed in [7]; and in [8], an adaptive model reduction method was presented and a moving horizon estimator (MHE) was designed. The model adaptation was performed every sampling time. This strategy together with the MHE estimation scheme made the method's computational complexity high.

In this work, we present an error-triggered adaptive model reduction method for state estimation of large-scale agro-hydrological systems. In the proposed approach, model adaptation is performed when the current reduced model is not sufficient to capture the dynamics of the system. To obtain a reduced model, state trajectories are first generated using irrigation information and rain forecast. Subsequently, an unsupervised clustering method is employed to obtain a projection-based reduced model. At each sampling time, the accuracy of the reduced model is evaluated using a moving horizon error indicator, which triggers online model re-identification when there is a significant deviation between the reduced model and the Richards equation. The purpose of the re-identification of the reduced model is to minimize the model-plant mismatch. An adaptive EKF is then designed based on the reduced model. Finally, the performance of the proposed method is compared to an EKF designed based on the Richards equation and an EKF based on a non-adaptive reduced model.

II. SYSTEM DESCRIPTION AND PROBLEM FORMULATION

A. System description

An agro-hydrological system represents the hydrological cycle of soil, crop, atmosphere, and water. The water infiltration in soil under the action of capillary and gravitational forces is characterized by the Richards equation [10]. A diagram of the agro-hydrological system is shown in Figure

Financial support from Natural Sciences and Engineering Research Council of Canada and Alberta Innovates is gratefully acknowledged. X. Yin acknowledges the financial support from Ministry of Education, Singapore, under its Academic Research Fund Tier 1 (RS15/21), and Nanyang Technological University (Start-up Grant).

Sarupa Debnath, Soumya Ranjan Sahoo, Bernard Twum Agyeman, and Jinfeng Liu are with the Department of Chemical and Materials Engineering, University of Alberta, Edmonton, AB, T6G 1H9, Canada. Corresponding author: J. Liu. Email: jinfeng@ualberta.ca

Xunyuan Yin is with School of Chemical and Biomedical Engineering, Nanyang Technological University, 62 Nanyang Dr, 637459, Singapore. Email: xunyuan.yin@ntu.edu.sg

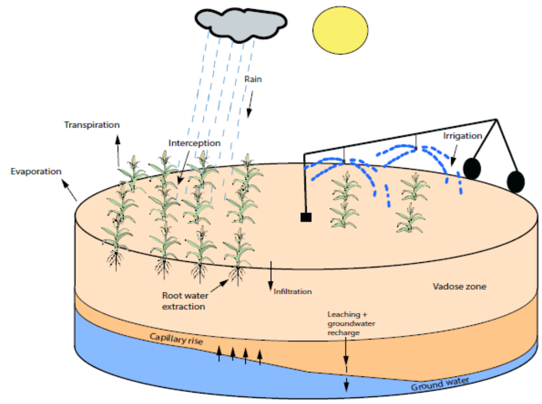

Fig. 1. Schematic of an agro-hydrological system [9]

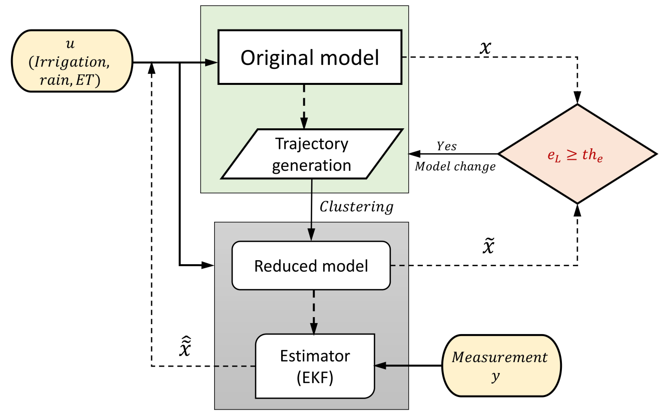

Fig. 2. The proposed model reduction and state estimation scheme

1 and the field is facilitated with a center-pivot irrigation system that rotates in a circular motion. To capture the movement of the center pivot, the Richards equation in cylindrical coordinate form is as follows [9]:

$$\frac{\partial \theta}{\partial t} = c(h)\frac{\partial h}{\partial t} = \frac{1}{r}\frac{\partial}{\partial r}\left[rK(h)\frac{\partial h}{\partial r}\right] + \frac{1}{r}\frac{\partial}{\partial \theta}\left[\frac{K(h)}{r}\frac{\partial h}{\partial \theta}\right] + \frac{\partial}{\partial z}\left[K(h)\left(\frac{\partial h}{\partial z}+1\right)\right] - S(h,z) \quad (1)$$

where h [m] is the field water pressure head, θ [m^{3}m^{-3}] is the field water soil moisture content, $c(h)$ [m^{-1}] is the soil water capacity, $K(h)$ [ms^{-1}] is the hydraulic conductivity, r [m], θ [rad], z [m] are the radial, azimuthal, and axial spatial variables, respectively, and $S(h,z)$ [m^{3}m^{-3}s^{-1}] is the sink term. The reader may refer to [8] for more details.

B. Problem formulation

We consider a continuous-time state-space model through the spatial discretization of equation (1) as follows:

$$\dot{x}(t) = f(x(t), u(t)) \quad (2)$$

where $x(t) \in \mathbb{R}^{N_x}$ denotes the state vector of the pressure head value of size N_x at each discretized node and $u \in \mathbb{R}^{N_u}$ represents the input vector of length N_u irrigation quantity at each discretized node at the surface. f defines the nonlinear system dynamics. At any given time, the center pivot irrigation system can only irrigate the nodes aligned with it, leaving the rest of the field unirrigated.

In this work, we assume the use of tensiometer sensors to measure the soil pressure head values at some selected nodes of the field at each sampling time. This considers the soil moisture observations at the surface as well as at various rooting depths. The measurements of these tensiometer sensors can be modeled as follows:

$$y(t) = Cx(t) + v(t) \quad (3)$$

where $y(t) \in \mathbb{R}^{N_y}$ denotes the measured outputs, C is a $N_y \times N_x$ matrix indicating the relation between x and the outputs and v denotes measurement noise. It is assumed that $N_y \ll N_x$ but still provides observability of the entire x.

Our objective is to estimate the soil pressure head x at the discrete nodes throughout the field by utilizing the measurement y. It is assumed that y is sampled with a sampling time Δ; that is, $y(t_k)$ with $t_k = k\Delta$, $k = 0, 1, \ldots$, are available. This is a standard state estimation problem except that the size of x can be very large. The large dimensionality of x typically leads to two challenges: (a) computational complexity of the model and the associated estimation schemes and (b) low degree of observability of x when the number of measured outputs is small. We propose to address these challenges by using an error-triggered adaptive model reduction method and design estimators based on the reduced model.

III. Proposed Adaptive State Estimation

In this section, we present the error-triggered adaptive model reduction method and the associated extended Kalman filter design. Figure 2 illustrates the essential steps involved in the proposed approach. The state-space model of Richards' equation (2) serves as the original model, and an error metric e_L is evaluated at each sampling time t_k to assess the accuracy of the reduced model against the original model by comparing their predictions of the system evolution. The metric e_L will be introduced later in equation (13). If the error metric exceeds a pre-determined threshold th_e set for the triggered criterion, a new reduced model is created to replace the previous reduced model. Soil moisture estimation of the entire field is done based on the reduced model and field measurements. The main components of the proposed approach are explained in the remainder of this section.

A. Adaptive model reduction

The implementation involves identifying a reduced model used for soil moisture estimation. At each sampling time, the metric e_L is computed, and if it surpasses the threshold th_e, the reduced model is re-identified. For model identification initially or upon e_L surpassing the threshold, identical steps are followed, outlined as follows:

Step 1: state trajectory generation: At a sampling time t_k, when the re-identification of the reduced model is triggered, the state trajectory of the original system (1) is generated. Specifically, the current state estimate at sampling time t_k is used as the initial condition, and the equation (2) is simulated with prescribed irrigation actions for total sampling intervals of N_{fd}. The trajectory of the state over the N_{fd} steps is denoted as $\mathscr{X}_m$ as follows:

$$\mathscr{X}_m = [x(t_k)\ x(t_{k+1})\ \ldots\ x(t_{k+N_{fd}})]^T$$

where $\mathscr{X}_m \in \mathbb{R}^{N_{fd} \times N_x}$ is the state snapshot matrix for the m^{th} model reduction assuming that there were $m-1$ model changes occurred before t_k. The reduced models that are generated during this process are expected to perform well for at least N_{fd} sampling intervals.

Step 2: clustering and reduced model generation: In this step, the new reduced model is created based on the snapshot matrix $\mathscr{X}_m$. Each column in $\mathscr{X}_m$ indicates the trajectory of a state element or a node x_i where i ($i = 1, \ldots, N_x$). The purpose of the clustering is to merge similar trajectories into one cluster. Instead of the state element x_i, a cluster will be considered as a state element of the reduced model. In this work, the agglomerative hierarchical clustering [11] is used. Initially, individual state elements are treated as clusters, and subsequently, the distances between these clusters are computed. Then, the clusters are merged such that the average distance is smaller than a threshold th_C. The average distance between two clusters is calculated as follows:

$$D(p,q) = \frac{1}{n_p n_q} \sum_{i=1}^{n_p} \sum_{j=1}^{n_q} d(x_{pi}, x_{qj})$$

where p and q denote the two clusters, n_p, n_q are the sizes of the clusters of p and q respectively, x_{pi} and x_{qj} denote data points within clusters p and q respectively.

Consider that after clustering, there are r_m clusters. Denote $C^{(m)} = \{C_1^{(m)}, C_2^{(m)}, \ldots, C_{r_m}^{(m)}\}$ as the collection of clusters for the m^{th} model reduction. The clusters satisfy the following two properties: i) $C_i^{(m)} \cap C_j^{(m)} = \Phi$ and ii) $C_1^{(m)} \cup C_2^{(m)} \cup \ldots \cup C_{r_m}^{(m)} = \mathscr{X}_m$.

The m^{th} reduced system is constructed based on the Petrov-Galerkin projection framework [12]. For the Petrov-Galerkin projection method, the projection matrix is required. The projection matrix ($U^{(m)} \in \mathbb{R}^{N_x \times r_m}$) is generated based on the clusters ($C^{(m)}$) and the elements of $U^{(m)}$ are expressed as follows:

$$U_{i,j}^{(m)} = \begin{cases} w_i, & \text{if point } i \in C_j^{(m)} \\ 0, & \text{else} \end{cases}$$

and w_i is determined as follows:

$$w_i = 1/||\alpha_i||,\ \alpha_i = \mathbb{E}_i^T \alpha$$

where $\alpha = [1, \ldots, 1]^T \in \mathbb{R}^{N_x}$, $||\alpha_i||$ is the L_2 norm of α_i, $\mathbb{E}_i = e_{C_i} \in \mathbb{R}^{N_x \times N_{C_i}}$ (N_{C_i} is the size of C_i) denoting a matrix whose columns are e_j's and each e_j is the j-th column of the identity matrix of size $\mathbb{R}^{N_x \times N_x}$.

The m^{th} reduced model of (2) is expressed as follows:

$$\dot{\xi}^{(m)}(t) = f_r^{(m)}(\xi^{(m)}(t), u(t)) \tag{4}$$

where $f_r^{(m)} = U^{(m)T} f$ and $\xi^{(m)}(t) = U^{(m)T} x(t)$. Note that the predicted state x from (2) can be approximated based on mapping $\tilde{x}(t) = U^{(m)} \xi^{(m)}$. After carrying out the numerical discretization, the discrete-time reduced-order model is as follows:

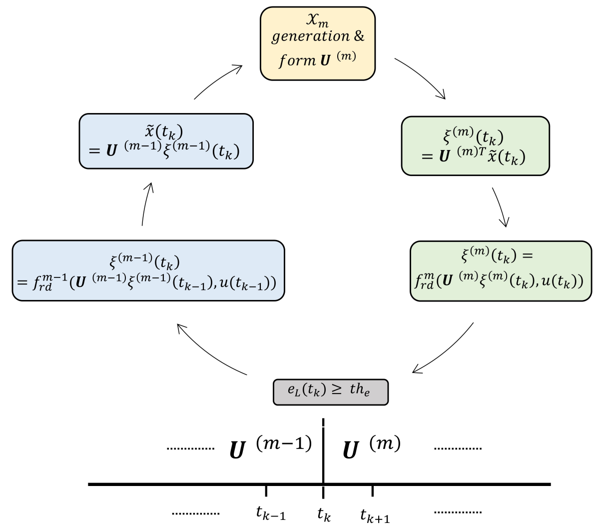

Fig. 3. Information exchange between reduced models

$$\xi^{(m)}(t_{k+1}) = f_{rd}^{(m)}(\xi^{(m)}(t_k), u(t_k)) \tag{5}$$

where f_{rd} is the discrete-time function of the reduced model. Note that when transitioning from one reduced model to another, the order of the new reduced model may differ from the order of the previous reduced model. To ensure a smooth transition between reduced models, the state information of the previous reduced model is mapped back to the full state and then the full state is projected to the new reduced model using the new projection matrix illustrated in Figure 3.

B. Adaptive extended Kalman filter

In this work, we design an estimator based on the adaptive model in the framework of extended Kalman filter (EKF). EKF is a commonly used filtering method for state estimation of nonlinear systems, which involves successive linearization of the nonlinear system. The advantage of using EKF is its computational efficiency [13].

In the adaptive reduced-order model framework, the standard EKF cannot be applied. To address this issue, we develop an adaptive EKF based on the adaptive model. Let us consider the discrete reduced model (5) with the corresponding output equation as follows:

$$\begin{aligned} \xi^{(m)}(t_{k+1}) &= f_{rd}^{(m)}(\xi^{(m)}(t_k), u(t_k)) \\ y(t_k) &= C_r^{(m)} \xi^{(m)}(t_k) + v(t_k) \end{aligned} \tag{6}$$

where $v(t_k)$ denotes the measurement noise at time k, $C_r^{(m)} = C\mathscr{U}^{(m)}$.

Adaptive EKF design: There are two steps in EKF: prediction step and update step. At the sampling time t_k, in the prediction step, the adaptive EKF first predicts the reduced state at t_k based on the state estimate at t_{k-1} and the reduced model as follows:

$$\hat{\xi}^{(m)}(t_{k|k-1}) = f_{rd}^{(m)}(\hat{\xi}^{(m)}(t_{k-1}), u(t_{k-1})) \tag{7}$$

where $\hat{\xi}^{(m)}(t_{k|k-1})$ represents the prediction of the reduced state at time instant t_k based on the estimated reduced state $\hat{\xi}^{(m)}(t_{k-1})$. The evolution of the variance of the process noise is also propagated based on the reduced model:

$$P_r^{(m)}(t_{k|k-1}) = A_d^{(m)}(t_{k-1})P_r^{(m)}(t_{k-1})A_d^{(m)}(t_{k-1}) + Q_r^{(m)} \quad (8)$$

where $P_r^{(m)}$ and $Q_r^{(m)}$ are the reduced covariance matrices for the state and process noise respectively, and $A_d^{(m)}(t_{k-1}) = \left.\frac{\partial f_{rd}^{(m)}}{\partial \xi^{(m)}}\right|_{\hat{\xi}^{(m)}(t_{k-1})}$ is the state-transition matrix obtained by linearizing the nonlinear reduced model at the estimated state at t_{k-1}. Note that if P and Q are the covariance matrices of the state and process disturbance for the original system, $P_r^{(m)} = U^{(m)T}PU^{(m)}$ and $Q_r^{(m)} = U^{(m)T}QU^{(m)}$.

At the sampling instant t_k, once the measurement $y(t_k)$ is available, it is used to update the predictions generated in the prediction step. This is the update step of the EKF. In the update step, an estimate of the current reduced state $\hat{\xi}^{(m)}(t_k)$ is obtained based on the predicted value $\hat{\xi}^{(m)}(t_{k|k-1})$ as follows:

$$\hat{\xi}^{(m)}(t_k) = \hat{\xi}^{(m)}(t_{k|k-1}) + K_r^{(m)}(t_k)(y(t_k) - C_r^{(m)}\hat{\xi}^{(m)}(t_{k|k-1})) \quad (9)$$

where $\hat{\xi}^{(m)}(t_k)$ represents the estimated reduced state at time t_k, and $K_r^{(m)}(t_k)$ is the correction gain used to minimize a *posteriori* error covariance based on the measurement innovation $y(t_k) - C_r^{(m)}\hat{\xi}^{(m)}(t_{k|k-1})$. The correction gain can be determined as below:

$$K_r^{(m)}(t_k) = P_r^{(m)}(t_{k|k-1})C_r^{(m)T}(R + C_r^{(m)}P_r^{(m)}(t_{k|k-1})C_r^{(m)T})^{-1} \quad (10)$$

where R is the covariance matrix of the measurement noise. The state covariance matrix is also updated as follows:

$$P_r^{(m)}(t_k) = (I_{r_m} - K_r^{(m)}(t_k)C_r^{(m)})P_r^{(m)}(t_{k|k-1}) \quad (11)$$

where $P_r^{(m)}(t_k)$ is the *posteriori* error covariance matrix of the estimation error at time t_k and I_{r_m} is an identity matrix of the m^{th} reduced model with size r_m. It is noted that $P(t_0)$, Q, and R are three tuning parameters for the EKF. The state estimate at the time t_k is $\hat{x}$ and evaluated from:

$$\hat{x}(t_k) = U^{(m)}\hat{\xi}^{(m)}(t_k). \quad (12)$$

Information exchange during model transition: When there is a model update, the information in the EKF based on the previous model should be smoothly transferred to the EKF based on the new reduced model. The information transfer is performed by mapping all the information back to the full state system and then projecting to the new reduced model. Consider that we need to transfer the information of the EKF based on the m^{th} reduced model to the EKF based on the $(m+1)^{th}$ model. The following steps are performed:

- Mapping the estimated reduced state and state covariance to the full order state and covariance: $\hat{x} = U^{(m)}\hat{\xi}^{(m)}$, $P = U^{(m)}P_r^{(m)}U^{(m)T}$.
- Projecting the full order information to the new reduced model using the new projection matrix: $\hat{\xi}^{(m+1)} = U^{(m+1)T}\hat{x}$, $P_r^{(m+1)} = U^{(m+1)T}PU^{(m+1)}$.

C. Design of the error metric e_L

The reduced model update or re-identification is triggered by an error metric e_L, which is evaluated every sampling time. Specifically, at t_k, the estimated state $\hat{x}(t_k)$ is considered as the initial condition. The trajectory of the system state over the next N_{f_d} steps is predicted both based on the original model of (2) and the current reduced model. It is assumed that the irrigation amounts of the next N_{f_d} steps are known, which is typically the case in agricultural irrigation. Once the predictions are generated, the deviation of the trajectory generated from the reduced model from the trajectory of the original full model is calculated and is used as the error metric e_L. The design of e_L is inspired by the work of [14] and is shown below:

$$e_L(t_k) = \frac{1}{N_x}\sum_{j=1}^{N_{f_d}}\sum_{i=1}^{N_x}|\tilde{x}_i(t_{k+j}) - x_i(t_{k+j})| \quad (13)$$

where $\tilde{x}_i$ and x_i denote the predictions of i^{th} state element using the reduced model and the original model respectively. A prediction horizon N_{f_d} is considered. A model reduction is triggered if $e_L(t_k)$ exceeds the predefined threshold th_e and subsequently a new reduced model is generated as discussed earlier.

IV. Application to an Agricultural Field

In this section, we demonstrate the effectiveness of the proposed adaptive model reduction and estimation in the state estimation of an agricultural field. The field is located to the east of Lethbridge, Alberta, Canada, with geographical coordinates ranging from Long: $-112.7385 : -112.7365$ and Latd: $49.6896 : 49.6908$. The field consists of a central pivot irrigation system, and the crop being grown is sugar beet in its growing stage.

The soil depth considered in this study is 0.4 m, which is discretized evenly into 12 nodes. The field has a radius of 50 m, which is discretized radially into 20 nodes and azimuthally into 40 nodes. The surface boundary condition is characterized by the Neumann boundary condition, which specifies the flow of water out of the system, and the bottom boundary condition is specified as free drainage. In this work, we assume the use of tensiometer sensors to measure the soil pressure head values at 90 selected nodes of the field at each sampling time, including surface nodes and nodes at various depths. The total number of nodes in the field is 9600. The discretized diagram of the research farm and the farm itself are shown in Figure 4.

The soil parameters in the field are known to vary across the field, as shown in Figure 5. In order to simulate the system, information about evapotranspiration (ET), crop coefficient (K_c), irrigation, and rain are used, as shown in Figure 6. The initial actual soil moisture x_0 in pressure head is simulated to be a distinct value for each quadrant of the field, namely, -3.5, -4.0, -2.7, and -1.5 m.

We consider three different estimation schemes to illustrate the proposed approach. Scheme I involves using the proposed adaptive modeling and EKF. In Scheme II, a reduced EKF is

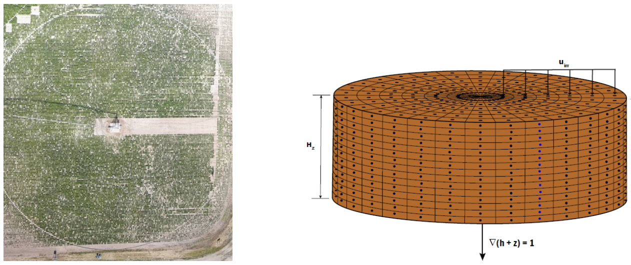

(a) (b)

Fig. 4. (a) Demo farm in Lethbridge, (b) A discretized diagram [8]

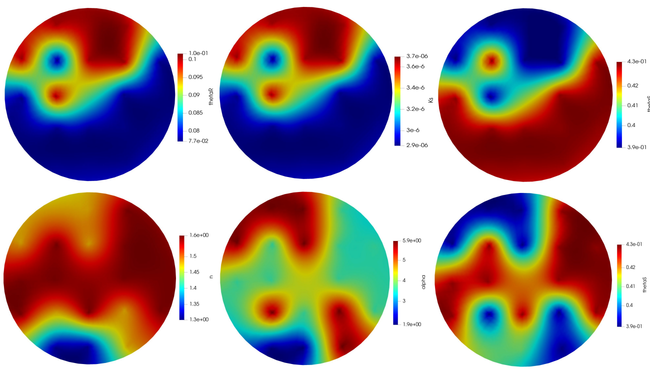

Fig. 5. Different soil parameters used in the simulation [8]

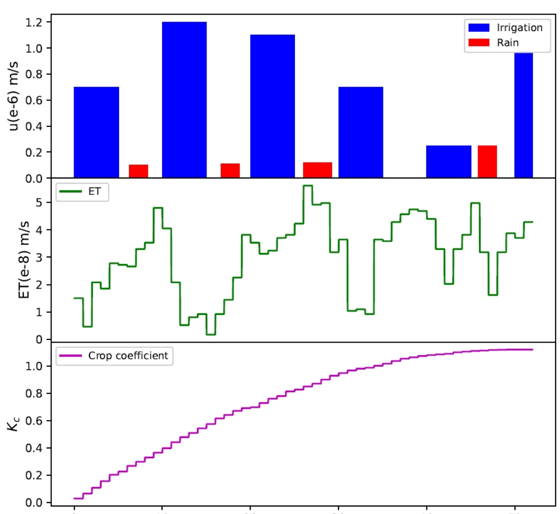

Fig. 6. Input (irrigation, ET and rain) and K_c to the system

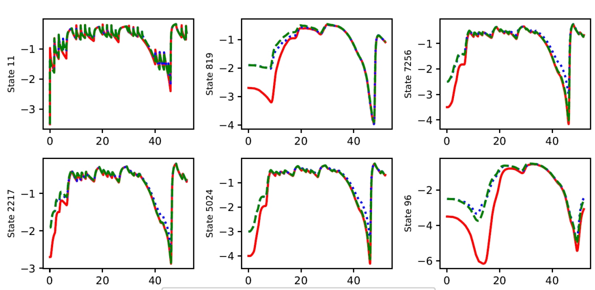

Fig. 7. Actual state trajectories and state prediction of schemes I and II

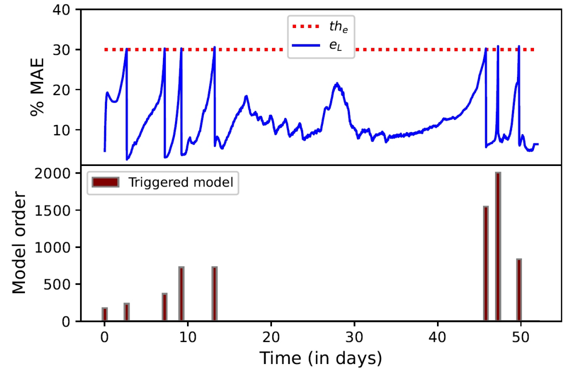

Fig. 8. The proposed error-triggered adaptive EKF Scheme I

designed based on a single non-adaptive reduced model. This approach assumes that all information, such as irrigation, Evapotranspiration (ET), and rain, is available for the entire growing season and is used to generate trajectories for the non-adaptive model creation. Finally, Scheme III involves a full-order estimator design based on a regular EKF, in which the original model is used. These three schemes will be compared to evaluate the proposed adaptive EKF's performance and determine its effectiveness in accurately estimating the entire field's soil moisture.

The simulation runs for a total of 52 days, and the initial guess for the soil moisture $\hat{x}(0)$ is set to -2.5, -3.0, -1.9, and -2.0 m for the four quadrants, which differ from the actual values of soil moisture $x(0)$. The units for the soil pressure head values are measured in meters (m). The covariance matrices Q and R are defined as identity matrices with diagonal elements of $Q = 1.0 \times I_{Nx}$ and $R = 0.08 \times I_{Ny}$, respectively. The initial state covariance matrix P has entries of 5×10^{-5} for all off-diagonal elements and a value of 1.0 for all diagonal elements. The measurement noise is considered normally distributed with a zero mean and a standard deviation of 0.1. The sampling time is $\Delta = 30$ min.

Note that the initial reduced model is generated based on the $\hat{x}(0)$ as the initial state and not the actual initial state $x(0)$. The $x(0)$ is only utilized to generate the actual trajectories of the system. In Figure 7, the trajectories of actual states and predicted states of schemes I and II are shown for a few selected states. The constant thresholds th_C for cluster generation are 0.2 and 0.5 in creating the new reduced model for scheme I and scheme II, respectively. Additionally, the non-adaptive reduced model used in Scheme II is found to be accurate enough at the order of 4708.

The proposed estimation approach, scheme I, employs a threshold $th_e = 0.3$ for the error-triggered criterion with $N_{f_d} = 48$. As depicted in Figure 8, the bottom plot displays the instances where error-triggered model re-identification occurred, with varying model orders. The re-identification is prompted by the error indicator e_L exceeding th_e. At the start and end of the simulation, frequent model changes were observed, with the highest model order of 2005 corresponding to high values of K_c and ET and a rapid decrease in the soil moisture.

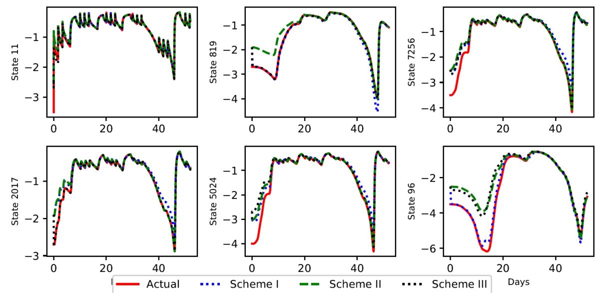

Fig. 9. Actual state trajectories and the state estimation of all schemes

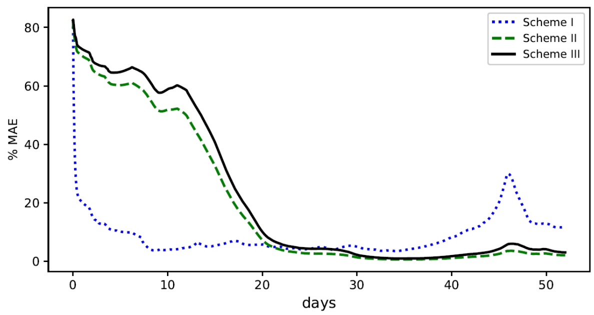

Fig. 10. State estimation performance of the schemes

In Figure 9, the actual state trajectories and state estimates for all schemes are shown to have excellent agreement with the system's actual trajectories. Figure 10 further highlights the percentage of the mean average error (% MAE) between the actual and EKF estimated states for all schemes. Note that the proposed scheme I converge much faster compared with the other two schemes may be due to the increased degree of observability of the estimation problem. In the proposed scheme, the number of measurements is kept the same (90) but the number of states that need to be estimated is significantly less. This helps the estimation scheme to converge faster. But at the same time, in the proposed approach, since each reduced model uses fewer nodes and the model mismatch error accumulates, the accuracy after the convergence is slightly poorer as can be seen from Figure 10. But with the triggered model adaptation, scheme I can maintain the estimation error within the pre-determined threshold through model adaptation. This can also be seen in Figure 10. The tuning parameters for re-identification of the reduced models include the fixed time N_{f_d}, threshold for cluster generation th_C, and error threshold th_e. These also provide more flexibility in tuning the estimation performance of the proposed approach.

The proposed approach is also much more computationally efficient. The error-triggered adaptive EKF scheme I, which includes adaptive clustering, model reduction, and recursive calculation, takes approximately 3 seconds to evaluate at each sampling time. Whereas, the non-adaptive reduced EKF scheme II utilizes a high number of reduced states, and takes longer for estimation, around 9 seconds per sampling time. It is worth noting that the assumption of having all information beforehand in the non-adaptive reduced EKF is not realistic, and subsequently, the system is prone to process and weather disturbances. Implementing the classical EKF based on the actual full-scale nonlinear model scheme III with 9600 discretization nodes is computationally challenging, and it takes approximately 35 seconds for each step. With an increase in the number of system states, the evaluation time for calculating the large state transition matrix A_d also experiences an exponential rise, rendering the estimation process computationally intractable, as indicated in [8].

V. Conclusions

In this paper, we addressed the problem of higher dimensionality of the agro-hydrological system equipped with a central pivot. We designed a reduced state estimator of the system based on an error-triggered model reduction method and implemented it in a real agricultural field. The proposed estimation scheme provides good estimates and improved the computation speed as compared to the non-adaptive reduced estimator and the full state estimator. Overall, the proposed estimation method is an effective solution for managing the complexity of large-scale agro-hydrological systems. For future work, we will consider the real sensor measurements in estimating soil moisture and apply the proposed method to a large-scale field.

References

[1] UN, "Waste water the untapped resource," *The United Nations World Water Development Report*, 2017.

[2] C. Lozoya, C. Mendoza, L. Mejía, J. Quintana, G. Mendoza, M. Bustillos, O. Arras, and L. Solís, "Model predictive control for closed-loop irrigation," *IFAC Proceedings Volumes*, vol. 47, no. 3, pp. 4429–4434, 2014.

[3] FAOSTAT, "Sustainable food and agriculture," 2020. 07 May, 2020.

[4] K. L. Moore and Y. Chen, "Iterative learning control approach to a diffusion control problem in an irrigation application," in *2006 International Conference on Mechatronics and Automation*, pp. 1329–1334, IEEE, 2006.

[5] X. Yin and J. Liu, "State estimation of wastewater treatment plants based on model approximation," *Computers & Chemical Engineering*, vol. 111, pp. 79–91, 2018.

[6] S. Debnath, S. R. Sahoo, B. T. Agyeman, and J. Liu, "Input-output selection for lstm-based reduced-order state estimator design," *Mathematics*, vol. 11, no. 2, p. 400, 2023.

[7] S. R. Sahoo, B. T. Agyeman, S. Debnath, and J. Liu, "Knowledge-based optimal irrigation scheduling of agro-hydrological systems," *Sustainability*, vol. 14, no. 3, p. 1304, 2022.

[8] S. R. Sahoo and J. Liu, "Adaptive model reduction and state estimation of agro-hydrological systems," *Computers and Electronics in Agriculture*, vol. 195, p. 106825, 2022.

[9] B. T. Agyeman, S. Bo, S. R. Sahoo, X. Yin, J. Liu, and S. L. Shah, "Soil moisture map construction by sequential data assimilation using an extended kalman filter," *Journal of Hydrology*, vol. 598, p. 126425, 2021.

[10] L. A. Richards, "Capillary conduction of liquids through porous mediums," *Physics*, vol. 1, no. 5, pp. 318–333, 1931.

[11] M. Steinbach, G. Karypis, and V. Kumar, "A comparison of document clustering techniques," *CS&E Technical Reports*, 2000.

[12] A. C. Antoulas, *Approximation of large-scale dynamical systems*. SIAM, 2005.

[13] S. Debnath, S. R. Sahoo, B. Decardi-Nelson, and J. Liu, "Subsystem decomposition and distributed state estimation of nonlinear processes with implicit time-scale multiplicity," *AIChE Journal*, vol. 68, no. 5, p. e17661, 2022.

[14] A. Alanqar, H. Durand, and P. D. Christofides, "Error-triggered online model identification for model-based feedback control," *AIChE Journal*, vol. 63, no. 3, pp. 949–966, 2017.